Meas. Sci. Technol. **11** (2000) 1792–1801. Printed in the UK PII: S0957-0233(00)14899-4

Non-contact acoustic microscopy

Matt Clark, Steve Sharples and Mike Somekh

School of Electrical and Electronic Engineering, University of Nottingham, University Park, Nottingham NG7 2RD, UK

Received 22 June 2000, in final form and accepted for publication 22 September 2000

Abstract. We demonstrate a fast all-optical surface acoustic wave (SAW) microscope. This acoustic microscope may be thought of as a non-contact (hence non-perturbing) surface acoustic microscope. The key to producing a sufficiently high SAW amplitude for imaging without producing surface damage is to tailor the generating optical distribution. This can be used to spread the optical power on the sample surface (preventing damage) and to focus the acoustic waves (increasing the amplitude). This paper discusses the general and specific design features of our microscope and important new developments in the general design of such instruments. Our microscope based on this technology is capable of producing high quality, quantitative images of SAW amplitude and phase (velocity) on many materials; this and new, unique, forms of acoustic contrast are demonstrated and discussed.

Keywords: acoustic microscopy, laser ultrasonics, ultrasound, scanning acoustic microscope, non-destructive testing/evaluation

1. Introduction

1.1. Scanning acoustic microscopy and non-contact methods

Acoustic microscopy techniques have many attractive features. In particular they are usually sensitive to the mechanical properties of the materials under inspection and contrast mechanisms reveal useful information about the physical structure of the sample. Conventional contacting scanning acoustic microscopes (SAMs) may be used to image surface acoustic waves on sample surfaces [1–3]. A problem with SAMs, however, is that a couplant (usually water) is required in order to allow acoustic waves to be coupled into the sample. The presence of the couplant is problematic in three ways; it can contaminate the surface of the material, it can perturb the measurement and it can restrict access to samples with complex geometries. The first may be a major reason why the SAM has not been adopted widely in some areas (for instance the semiconductor industry). The second is a major bar to the use of SAMs for making quantitative measurements (of velocity and attenuation) and for revealing certain types of contrast. The third may restrict examination of real industrial components such as turbine blades. In addition to these three problems, there are advantages in being able to make remote measurements in many circumstances in which direct contact with the sample may be difficult to achieve or hazardous.

2. Optical techniques

2.1. Optical generation

Acoustic waves are usually optically generated in materials by thermoelastic or ablative stresses. The mode and frequency content of the acoustic waves generated primarily depends upon the temporal frequency content of the laser light and the spatial distribution of the light on the material (sample) surface [4, 5].

At high optical powers it is possible to generate relatively high acoustic amplitudes; however, it is easy to damage most materials through ablation or melting. Surface damage need not be important in many experiments (in some cases the surface effects can even be beneficial). In this paper we will consider that any surface damage would be unacceptable for a practical non-contact SAM.

2.2. Optical detection

There are many optical detection techniques; the commonly used devices in laser ultrasonics include various interferometers (sensitive to the displacement or velocity of the surface) and knife-edge detectors (sensitive to the tilt of the sample surface). A recent development is the use of photoemf receivers together with various optics to form either interferometers or knife-edge detectors [6]. When they are used with care, most of the techniques have broadly similar detection sensitivities [4, 7].

2.2.1. Rough surfaces. In addition to their relative insensitivity, optical techniques need to be applied with care on optically rough surfaces. There are approaches allowing detection on optically rough surfaces; for instance, using the Fabry–Pérot interferometer [7]. In this paper this is not a particularly important consideration because typical samples are optically smooth and consequently the detection techniques used (knife-edge) have been chosen for simplicity and effectiveness at high frequencies. We note also that, as the wavelength of the ultrasound begins to approach the

optical wavelength, an optically rough surface would also begin to appear acoustically rough.

2.3. Signal levels

Compared with contacting transducer techniques, all of these optical detection techniques are relatively insensitive [4, 8]. Typically the sensitivity is one or two orders less than those of contacting transducer techniques [4]. The lack of sensitivity of optical detection techniques presents a particular problem for all-optical acoustic microscopes because the speed of measurement is important.

We note that the signal-to-noise ratio (SNR) of an all-optical system in the thermoelastic regime is proportional to $P_{gen}\sqrt{P_{det}}$, where P_{gen} is the optical power used to generate the acoustic wave and P_{det} is the optical power used to detect it [4, 5]. This is an important result in that it indicates that much more can be gained, in terms of SNR, by increasing the total generation power rather than the detection power. It is usual that the main limitation on the amount of generation power used is the possibility of surface damage while the main limitation on the amount of detection power used is usually financial cost. Using tailored generation distributions helps to overcome the limitation associated with the risk of damage, allowing the SNR to be increased by the use of more generation power.

3. All-optical acoustic microscopy

3.1. Generic all-optical ultrasound systems

In a general all-optical ultrasound system there are usually separate transmission (generation) and reception (detection) systems. This may be contrasted to contacting ultrasonics, for which it is common for a single transducer to be used as transmitter and receiver. It is usual that the generation and detection systems use separate lasers. The generation laser is generally of high power and equipped to produce short pulses. The upper frequency limit of ultrasound is usually determined by the temporal frequency characteristics of the generating laser and the spatial characteristics of the illumination distribution on the sample surface†. The detection laser is generally a continuous wave laser of lower power and may have some special characteristics depending on the detection method used (for instance a narrow spectral line width would be used in a Fabry–Pérot detector).

Figure 1 shows a typical all-optical acoustic measurement set-up. It is possible for the optics to be relatively remote from the sample, depending on the frequency and type of acoustic waves studied. The stand-off distance between the optics and the sample ultimately depends on the required spatial resolution of the optical distributions on the sample surface. When the required resolution is high the stand-off distance is reduced. As a rule of thumb the required resolution is determined by the need to resolve half the effective ultrasound wavelength at the sample surface‡. For bulk waves travelling into the sample the effective wavelength is large so

† At very high frequencies (a few gigahertz) other limiting mechanisms come into play, such as the thermal diffusivity of the material.

‡ The effective wavelength is the distance between wavefronts at the sample surface and is always equal to or greater than the actual wavelength.

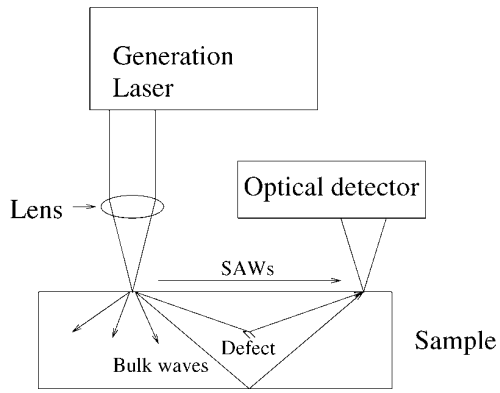

Figure 1. A generic all-optical ultrasound system. This shows separate send and receive systems and a variety of wavemodes and paths between generation and detection.

the stand-off distance can be large even at high frequencies because the waves intersect the surface obliquely. For surface waves the effective wavelength is the same as the actual wavelength and the stand-off distance is determined by the need to resolve the acoustic waves.

Generation and detection can be performed at the same point on the sample, separated points on the same surface or separate surfaces depending on the required acoustic geometry. However, detecting at the point of generation can cause problems for some experiments because the sample surface can be perturbed by the localized heating§. In figure 1 the optical element used to control the distribution of light on the sample is typically a lens, which is used to concentrate the light onto a small area to increase its power density on the sample surface [9]. Many techniques use a cylindrical lens to produce a line focus instead of a spot, which can reduce the optical power density on the sample surface and improve the directivity of the ultrasound generated.

In general the optical generation source will produce longitudinal and shear bulk waves and surface waves. The directivity pattern and frequencies of the waves generated depend on many things, including the distribution of generating light on the sample surface. This dependence of the modes generated on the optical distribution can be utilized to improve the performance of an all-optical SAM. This is the approach we have exploited to produce an all-optical SAM that is capable of fast non-contact and damage-free acoustic imaging.

3.2. Coping with poor detection sensitivity

The relative insensitivity of optical detection techniques is the dominant problem for non-contact acoustic imaging. The two common techniques used to improve signal-to-noise levels are averaging of signals and the use of large generation powers. Both of these techniques are problematic for a SAM; the former because it slows the experiment down and is relatively expensive, requiring high speed digital capture of data, the latter because it is easy to reach the damage threshold of many materials before the limit of single-shot detectability is reached. Thus, to cope with two major requirements

§ Optical cross talk between generation and detection systems can also make this difficult.

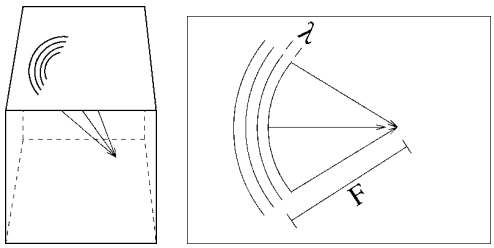

Figure 2. Schematic tailored generation patterns for bulk (*a*) and surface (*b*) waves, the line spacing is one (effective) wavelength.

of an all-optical SAM microscope (fast and non-destructive acquisition of images) another approach is needed, in order to improve the signal levels so that the single-shot SNR of the detection system is greater than unity.

3.3. Tailored generation profiles

By tailoring the optical distribution used to generate the ultrasound particular modes, frequencies and spatial distributions of ultrasound can be excited. This technique can also be used to distribute the generating light over a large area because the light can be placed at any location on the sample surface that adds ultrasonic amplitude to the required mode rather than in just one line or spot. Focusing the acoustic waves onto the detection point increases the detection signal by combining all the generated amplitude into a small area (or volume). This is most easily done by shaping the generating light into an arc†. This also spreads the generating light over a large area, reducing the peak intensity (figure 2). By using several arcs rather than one, the peak intensity can be further reduced without reducing signal levels (although the bandwidth of the acoustic signal may be reduced).

The number of arcs that may be used is ultimately limited by the requirements of the particular application. The limitation may be the required acoustic bandwidth, the physical limits on the size of the distribution of the generating light, the velocity tolerances or ultimately the absorption within the material which will prevent the arcs furthest from the focus contributing to the signal. The velocity tolerance is often the most important because the line spacing has to be matched to the sample velocity so that the first and last lines add up in phase. With many lines, this requirement becomes difficult to achieve, especially on inhomogeneous materials. Furthermore, the material at the point of generation is perturbed by the localized heating, so very accurate velocity matching (to within better than 1%) can be difficult in practice. The enhancements of signal level that can be achieved depend principally on the required bandwidth of the signal, the acoustic wavelength and the physical size of the acoustic part of the experiment (the width and propagation distance).

3.3.1. Improvement factors. For surface waves an approximate expression for the increase in acoustic amplitude

† Arcs are used for *flat* and *isotropic* or *effectively isotropic* materials. *Anisotropic*, *curved* or *aberrating* materials may require other shapes.

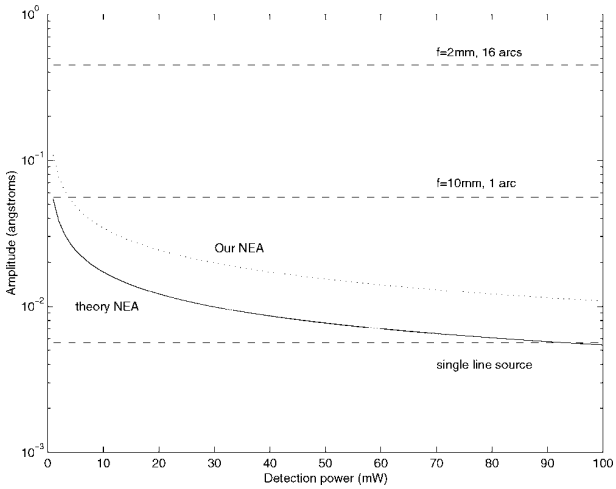

Figure 3. A graph showing the theoretical noise equivalent amplitude (NEA) for a knife-edge detector (solid line) after [4], using a bandwidth of 10 MHz. The dotted line is for a 'practical' NEA of twice the theoretical for our system. The horizontal broken lines describe the theoretical amplitudes for three different generation distributions each using a maximum intensity of 200 GW m^{-2} (the typical ablation/melting limit [4]) for our typical system (see section 5) calculated using [5]. The lower broken line indicates the amplitude generated by a single line source, the middle line shows that for a single arc (focal length 10 mm) and the upper line shows that for 16 arcs with a mean focal length of 2 mm. Where the curved lines intersect the straight the signal-to-noise level may be expected to be about unity for that detection power and generation source; when they fall below this the SNR is higher.

achieved by focusing the waves using an arc compared with the amplitude generated using a line source is

$$A_{focus} = \frac{x}{(2\lambda_{SAW}F)^{1/2}} \tag{1}$$

where x is the length of the line source or arc, λ is the acoustic wavelength, F is the working distance between the line or arc and the detection point (the focal length of the arc) and $x \gg \lambda$ and $x > (2\lambda_{SAW}F)^{1/2}$ so that the arc may be regarded as a true focusing element. This is derived using simple scalar diffraction theory [9].

Assuming that surface damage is the primary limitation on the optical power used, the signal can be further increased by using as many arcs (N_a) as the fractional bandwidth of the signal required (or other restriction) permits. The fractional bandwidth can be given as $W_{frac} \approx N_a^{-1}$ and the improvement factor of the signal can be given as $A_a = N_a = W_{frac}^{-1}$. However, this is only approximate and assumes that all the arcs are the same length and that the required fractional bandwidth is the only restriction on the number of arcs used.

Figure 3 shows the noise equivalent amplitude for a knife-edge detector (after Scruby and Drain [4]; note that this is typical of most detection techniques) against the detection power. The expected Rayleigh wave amplitudes for three differently shaped sources for aluminium are shown as horizontal broken lines (calculated using [5] and equation (1)). Each of the sources is calculated using the same peak intensity of around 200 GW m^{-2} for our typical system (see section 5), the ablation/melting limit [4]. It

can be seen that, with an arc or multi-arc source, detection can be performed with a SNR of more than unity even at quite modest detection powers, whereas the single line source would require averaging even at quite large detection powers.

As noted in section 2.3, the SNR is proportional to the generation power and the square root of the detection power. Figure 3 shows that this can have a dramatic effect on the detectability of the signal (an improvement in signal levels of 80-fold is equivalent to using more than 5000 times more detection light). It is important to note that damage-free measurement with a simple single line source requires the use of signal averaging†, which makes imaging difficult because of the measurement speed.

For bulk waves the situation is more complicated and depends strongly on the geometry of the experiment. Since it is not generally possible to focus the acoustic waves both at the region of interest and in the detection region simultaneously (as with surface waves and contacting transducers), it is not usually possible to use the generated ultrasound as efficiently as with surface waves. Tailored detection using many points to pick out a particular mode is possible but improvements of signal level are harder to achieve because of the $\sqrt{P_{det}}$ dependence of the SNR of the system on the total detector power. In addition the limitation on the amount of detection light used is usually economic rather than the need to limit damage. Thus using more detection points does not usually mean using more light and therefore does not give any gain in sensitivity.

4. A general all-optical SAM with focused ultrasound

Any all-optical SAM would incorporate some measure to ensure that the detectability of the SAW signal was high enough to allow imaging within a reasonable time. Figure 3 shows that simple tailoring of the generation optical distribution can have a dramatic effect on the detectability because the SAW amplitude is proportional to the generating power while the SNR is proportional to the square root of the detection power. This allows the limit of single-shot detectability to be reached while remaining in the thermoelastic regime and thus avoiding surface damage of the sample. It shows that better overall signal levels can be achieved using focused generation with 10 mW of detection power than a line source with 1 W of detection power (around the CW damage limit for a focused optical spot in many cases).

This, of course, is a simplification because the details of the damage thresholds for any particular system would depend ultimately on many parameters, not just the peak power. However, it is evident that, using modest repetition rates and modest average powers, the use of tailored generation distributions allows damage-free all-optical surface acoustic microscopy.

4.1. Controlling the generation distribution

There are various methods for controlling the distribution of light on the sample surface (see table 1). Most of these are not capable of producing arcs or multiple arcs and some of them are difficult to use in practice. From table 1 it is clear that computer generated holograms (CGHs) and spatial light modulators (SLMs) offer the most flexibility in designing optically generated acoustic elements. CGHs have some unique advantages (for instance the generation of three-dimensional distributions) but it is not currently possible to produce holograms that can be changed in real time‡. SLMs offer many of the advantages of CGHs and can change in real time so that many different acoustic elements can be generated easily and different material velocities can be matched easily.

5. A non-contact SAM in practice

We have constructed an all-optical SAM based on this general idea of improving signal levels by tailoring the distribution of the generating light. Figure 4 is a schematic diagram of the system and figure 5 shows an unaveraged SAW signal received by the detector. The acoustic frequencies are determined by the generation laser. This is a Q-switched, modelocked laser, producing a tone-burst of approximately 30 very short pulses (200 ps) separated by 12.1 ns with a variable repetition rate (up to 5 kHz). The average power output of the laser is around 2 W (depending on the repetition rate); at low repetition rates (below 2 kHz) the peak power reaches a maximum, whereas above this it decreases with increasing repetition frequency. The signal has a fundamental frequency of 82 MHz and contains harmonics of this. The current system can form images at 82 and 164 MHz. Higher frequencies have been observed but are currently beyond the upper bandlimit of the electronics and optical distribution used in the system, although these are not fundamental limits.

The bandwidth of the signal is around 5 MHz. In order not to narrow this bandwidth, the maximum number of lines or arcs used must not exceed about 16.

The microscope currently uses various computer generated holograms [13] to tailor the optical distribution on the sample surface and is being converted to use a SLM. The stand-off distance from the optics to the sample is around 50 mm, which is determined by the need to resolve the SAWs at 164 MHz ($\lambda \simeq 20\ \mu$m in Al).

Holograms that produce 1–16 arcs with focal lengths of 1–10 mm have been fabricated with arc spacings to match velocities of various materials from 3000 m s^{-1} (Al) to 5700 m s^{-1} (silicon nitride). The arc spacing of any particular hologram can be finely tuned using a simple optical zoom system to closely match the SAW velocity. In addition to these basic designs, holograms to generate distributions that can high or low pass or bandpass filter the generated SAWs have been made and we have also produced holograms that produce diffractive acoustic elements, which can produce complex focal distributions and frequency dependent distributions [14]. These are useful for examining a material at one frequency without any background at another and for looking for harmonics

† Unless very large detection powers are used.

‡ Some systems do offer the possibility of real-time CGH generation but these are currently too limited in spatial bandwidth to be practical; additionally the design methods are too slow for many applications.

Table 1. Optical elements for the control of laser ultrasound.

Technology	Advantages	Problems
Lens	Simple and available	No control
Cylindrical lens	Simple and available	Restricted control
Fixed grating	Some mode control	No focusing
Moving grating [10]	Efficient	Difficult to use, no focusing[a]
Axicon [11, 12]	Simplicity	Restricted geometry, fabrication difficult
Computer generated holograms	Arbitrary shapes, focusing, multiple arcs and three-dimensional shapes and surfaces	Fabrication difficult, fixed in time
Spatial light modulator	Arbitrary shapes, continuous control, flexibility and control and adaption	Power handling and control

[a] It is possible to combine a diffractive optical element with a frequency shifted beam to produce a moving circular grating, although control would be difficult.

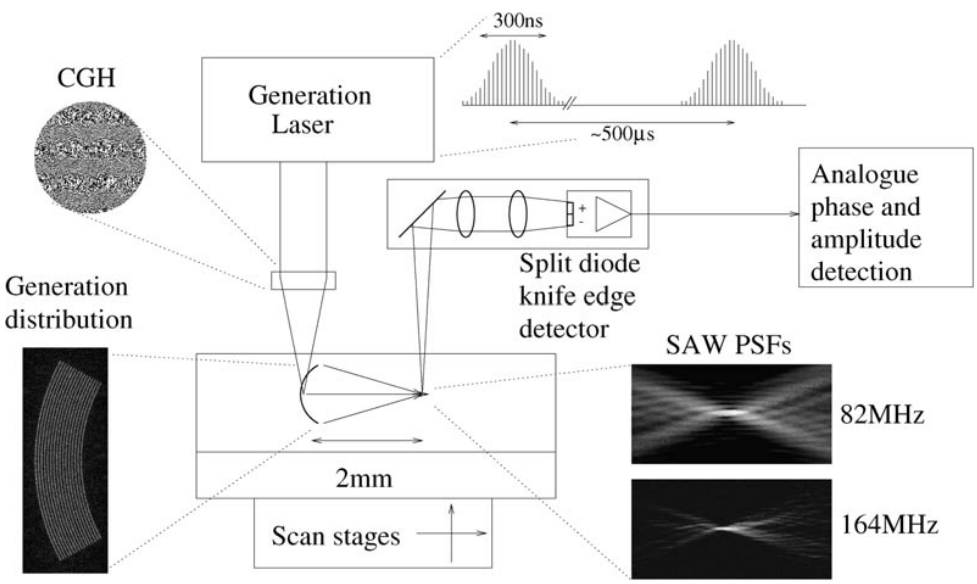

Figure 4. A schematic diagram of an all-optical SAM operating at 82 and 164 MHz. The generating laser is a 2 W (average power), Q-switched, modelocked lamp pumped Nd:YAG laser with a Q-switching frequency of 0.1–5 kHz and a fundamental modelocking frequency of 82 MHz. It produces a tone burst of 30 short pulses separated by 12.1 ns every 500 μs. A computer generated hologram (upper left-hand-side inset) is used to produce 16 arcs with a mean focal length of 2 mm on the sample (lower left-hand-side inset), the separation of the arcs depends on the material velocity, in this case it is $\approx$37.5 μm, which is suitable for aluminium and glass. A SLM generation system is currently under development. The lower right-hand-side inset shows the SAW point spread functions (PSFs) measured at the focus. The detector is a knife-edge design using a split photodiode and differential rf amplifier instead of a simple knife edge. The signals are captured in a simple phase and amplitude measuring system. The phase is measured with respect to a reference signal from the generating laser's modelock driver (which is coherent with the laser pulses). The sample and the detector are mounted on scanning stages. This allows the sample to be scanned to build up an acoustic image of the sample and the detector to be scanned to examine the distribution of ultrasound resulting from the generation distribution.

generated by nonlinearity of a material [15] rather than by the generating laser.

Without focusing it would be usual to average the waveforms 1000 times to improve the signal-to-noise level. Using a digital oscilloscope, this typically takes around one minute per measurement point, which is clearly too slow for imaging purposes.

5.1. Signal levels

The power densities for this system were chosen experimentally so that no surface damage results from prolonged exposure (many hours) for any of the materials tested. However, despite this lack of surface damage, glass samples were found to occasionally fracture after prolonged exposure because of dc heating. This can be avoided by gentle air cooling of the sample. (The total heat dissipation required is generally much less than the maximum 2 W because most of the optical power is reflected by the sample.) The typical peak optical power density used is 200 GW m^{-2} (along the lines or arcs), roughly corresponding to the melting/ablation limit in [4].

Using a 60° arc with a focal length of 2 mm, the heating in the generation region was not found to perturb the detection area. However, the dc heating was found to cause the measured phase of the signal to drift slowly over time as the region between generation and detection warmed; again this can be avoided with gentle air cooling. Using the full power

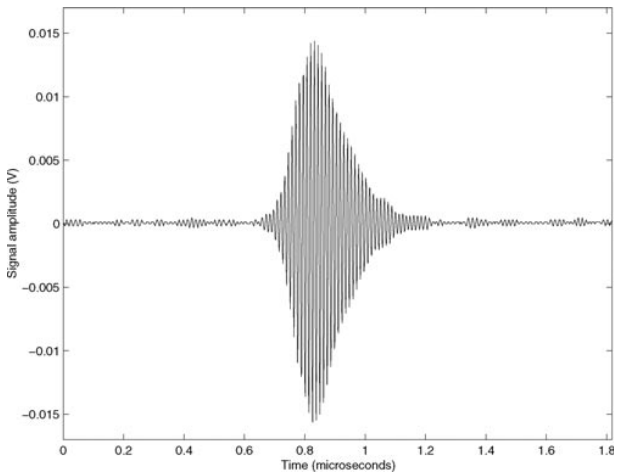

Figure 5. Unaveraged 82 MHz SAW waveform captured on an 'ideal' sample made from aluminium coated glass. The SAW was generated using a 16-arc source with a focal length of $\simeq$2 mm. It was detected using a knife-edge detector at the focal region using approximately 20 mW of light at 532 nm wavelength. No damage was observed on the sample after prolonged exposure to the system. The signal was filtered electronically with a bandwidth of approximately 20 MHz. The amplitude is about 80 times higher than it would be for a single line generation source of the same intensity.

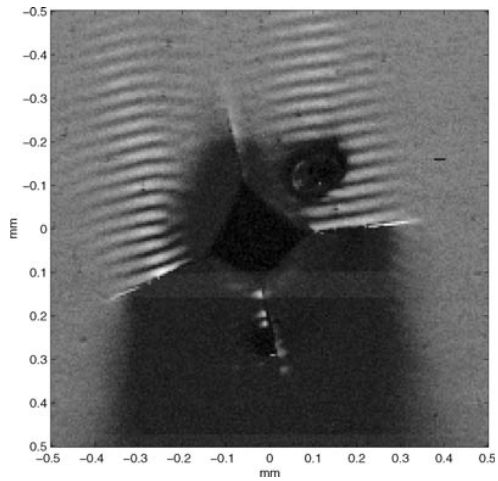

Figure 6. In this image the 82 MHz SAW is propagating from top to bottom on a silicon nitride sample. The defect in the centre is caused by a Vickers hardness indentation which has cracked the surface (four cracks radiating out from the corners of the indentation). The horizontal fringes are caused by a strong SAW reflection from the cracks (indicating that they are nearly normal to the surface). The SAW wavelength is 70 μm and the pitch of the reflection fringes is 35 μm. Little SAW amplitude gets past the cracks. Note the presence of small patches of large amplitude at the crack edge and along the lower central crack; these are anomalous in the sense that the presence of the SAW alone is not enough to explain them.

of our laser with an acoustic focal length of 2 mm, 16 arcs were required in order to remain in the damage-free regime; this is the maximum number of arcs our system can support without reducing the bandwidth of our signal significantly. Figure 5 shows an unaveraged signal taken on a mirror coated glass sample using approximately 20 mW of detection light. The focusing of the SAWs using these 16-arc holographic elements produces, at the focus, acoustic amplitudes about 80 times greater than that of a single line with the same optical intensity.

It is clear from figure 5 that it is possible to capture the signal using analogue electronics without any averaging. Hence it is possible to make measurements on every Q-switched pulse from the generating laser, which gives this system a maximum measurement rate of 2 kHz, corresponding to the Q-switching repetition rate. In practice the generating laser output varies slightly from pulse to pulse and it is usual to average 5–10 measurements after analogue capture at each scan point. It would be possible to normalize the measurements by capturing the output from the generation laser; however, the principal limit on the measurement rate is currently the speed of the scanning stages rather than the laser repetition rate.

6. Acoustic imaging results and contrast mechanisms

6.1. The amplitude response

Figure 6 shows a SAW amplitude image taken on a piece of silicon nitride at 82 MHz (wavelength 70 μm). The central defect was caused by a Vickers hardness indentation which has cracked the surface. The propagation direction of the SAW is from top to bottom. The contrast results from the scattering of the SAWs by surface or near surface defects in the mechanical structure of the sample. In figure 6 strong interference fringes can be seen where the SAW is scattered off cracks radiating out from the hardness indentation. There is a shadow region behind (below) the crack where the SAWs have been blocked. The fringes have a modulation depth of nearly unity, indicating that the amplitude of the reflected wave is nearly the same as that of the incoming wave. This indicates that the crack is deep compared with the SAW wavelength and nearly normal to the surface and that there is little mechanical contact between the crack walls. There are some anomalous features in this image, a region of high amplitude along the crack edge and some regions of high amplitude in the SAW shadow region (along the edge of a crack running vertically). The presence of these regions cannot be explained by the presence of Rayleigh SAWs alone and indicates the presence of other modes.

This image was taken using the non-contact SAM with a CGH optical element that produces four 60° arcs separated by 70 μm with a mean radius of 10 mm. The image is made up of 40 000 measurement points and was taken in around 20 min. The primary limitation on the measurement rate was the velocity of the stages. At the current measurement rate the imaging time would be around 4 min.

6.2. Multi-frequency response/sectioning

Figure 7 shows the same sample and defect as were shown in figure 6 imaged using 164 MHz SAWs. Many of the same features are visible, strong reflection fringes and a distinct shadow region. The fringes and the shadow region extend further out from the centre of the defect at 164 MHz than they do at 82 MHz. The crack is thought to become shallow at its

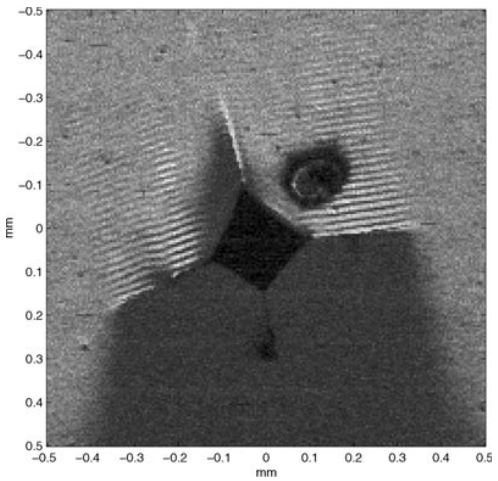

Figure 7. This image shows the same feature as that in figure 6 imaged at 164 MHz. The SAW wavelength is 35μm and the pitch of the reflection fringes is 17.5 μm. Note that the apparent width of the horizontal cracks is greater than it was at 82 MHz. This is thought to indicate that the cracks become shallower towards their edges, giving a weaker response at 82 MHz than at 164 MHz at the edges. This results from the shorter penetration depth of SAWs at higher frequencies.

edges and this means that the longer wavelength (82 MHz, which penetrates deeper into the surface) can travel beneath the shallow ends of the crack while these still block the shorter wavelength 164 MHz waves.

The use of multiple frequencies allows sectioning of the material near the surface. The velocity differences among various frequencies may also be used to determine coating properties near the surface, for instance the coating thickness or surface stress.

6.3. Lamb wave contrast

Figure 8 shows a sub-surface void imaged with the non-contact SAM. The depth of the void changes on going from left to right (it is deeper on the left-hand side) and distinctive Lamb wave fringes can be seen over the surface of the void. The fringes are caused by interference from the two lowest order modes, A_0 and S_0, which are strongly excited by the incoming SAW (Rayleigh wave). The pitch of the fringes changes with depth because the speed of the Lamb modes changes as the thickness of the layer in which they are travelling changes. The velocities of the individual modes can be inferred from the phase of the signal or from the pitch of the fringes, which can be used to calculate the velocity difference and therefore the individual velocities. This can be used to determine the thickness of the material covering the void.

This form of contrast would be hard to achieve in a conventional SAM because the couplant would damp the Lamb modes (especially the asymmetrical mode). This can be seen in the lower image of figure 8, in which the back of the void has been filled with water. In this image the Lamb modes are heavily attenuated by the presence of the water and the fringes die out quickly across the void. In this way the non-contact SAM can be seen to be sensitive not only to the presence of subsurface defects but also to their nature.

6.4. The phase response

Figure 9 shows phase amplitude and phase contrast on a piece of aluminium. There is a subsurface void which cause the SAWs to undergo mode conversion into Lamb waves over the void (see section 6.3), which can be seen as distinctive fringes (left-hand image). Because the Lamb modes have different velocities, the phase of the detected waves changes over the void. This can be seen as a distinctive change in the phase in the right-hand image. The gradient of the phase can be related to the small velocity changes δv in the sample by

$$\frac{\delta v}{\bar{v}} = \frac{1}{k_R}\frac{\partial \theta}{\partial z} \tag{2}$$

where $\bar{v}$ is the mean velocity, k_R is the SAW wavenumber (at the mean velocity) and $\partial\theta/\partial z$ is the phase gradient. It can be seen from figure 9 that the phase in this case is not smoothly varying (apart from the phase wraps), due to the presence of more than one acoustic mode.

Figure 10 shows the unwrapped phase of the first and last scan lines of the data shown in figure 9. These scan lines were chosen because over the void they are dominated by just one Lamb mode, making the graphs easier to interpret. By fitting a straight line to the phase of the dominant Lamb mode, the phase gradient can be measured and the change in velocity can be measured directly. Figure 10 gives a value of the velocity difference of -280 m s^{-1} (maximum) for the A_0 mode and of 700 m s^{-1} for the S_0 mode (minimum) relative to the Rayleigh velocity. In this case the velocity difference cannot be considered small enough for equation (2) to be particularly accurate; also the presence, in this case, of more than one acoustic mode makes it difficult to determine the phase gradient.

Since the full complex amplitude of the SAWs is captured in this system, the presence of the various modes can be shown by Fourier transforming the complex amplitude distribution along the direction of propagation. This separates the velocity components in spatial frequency space and allows the velocity of each component to be measured.

Figure 11 shows the data shown in figure 9 Fourier transformed along the direction of propagation. The spatial frequency axis (vertical) has been transformed to show velocity. This image shows three distinct bands, indicating the presence of three wavemodes travelling at different velocities. The broken lines marked on the image show the Rayleigh and Lamb velocities fitted to the data using the solutions for the Lamb wave velocities from Viktorov [16]. The velocities of the Lamb modes depend on the thickness of the material over the void, which can be inferred from the fitting of the Lamb wave data. In the case of figure 9 the thickness of the material is measured as 31 ± 2 μm on the left-hand side, decreasing to 25 ± 2 μm on the right-hand side. This technique for measuring the thickness of such a void is promising for thicknesses from around $0.1\lambda_{SAW}$ to around $2\lambda_{SAW}$, depending on the size of the void. At large thicknesses a large void is required in order to resolve the two modes; at lower thicknesses it may be difficult to excite sufficient amplitude in both modes to perform an accurate measurement.

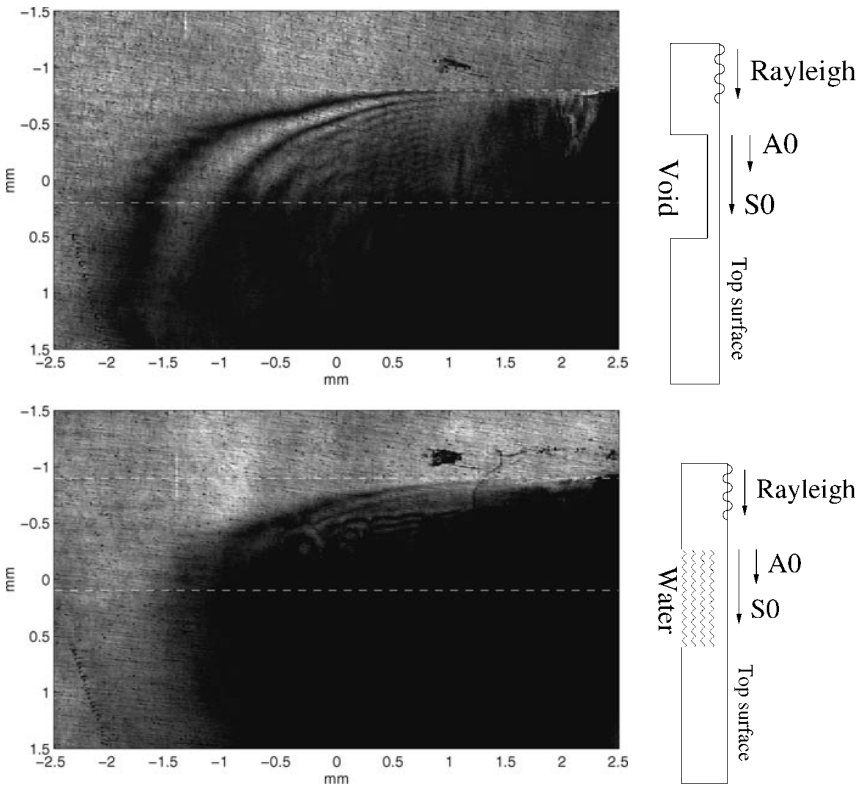

Figure 8. An example of Lamb wave contrast. Both pictures were taken of the same sub-surface void (marked with a broken line) on a piece of aluminium using 82 MHz SAWs. The depth of the void changes on going from left to right and distinctive Lamb wave fringes can be seen on the void. The fringes are caused by the interference of the first symmetrical and antisymmetrical Lamb modes excited by the Rayleigh wave. The lower image exhibits fewer fringes and a lower total amplitude over the void. In this case the void was backed with water (rather than air), which has damped the Lamb modes (especially the asymmetrical mode). The sample was fabricated by milling a slot into the back surface of a 3 mm thick aluminium plate at a shallow angle to the front surface. The depth of the void can be inferred from the angle and the point at which the void breaks the surface.

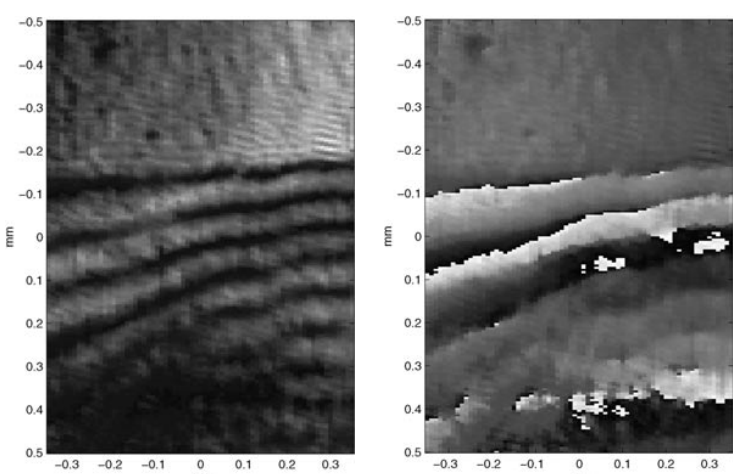

Figure 9. The image on the left-hand side shows the SAW amplitude at 82 MHz on a piece of aluminium with a subsurface defect (for details of the defect see figure 8). The image on the left-hand side shows the SAW phase. The SAW is travelling from top to bottom and the phase wraps at 2π boundaries in this direction. A constant phase indicates constant velocity; a changing phase indicates a change in velocity. The change in velocity is related to the gradient of the phase. The phase image is complicated by the presence of more than one acoustic mode (see section 6.3). These modes can be observed by taking the Fourier transform of the complex amplitude of the SAW along the direction of propagation (see figure 11 later).

7. Current progress

Compared with accepted transducer techniques, the all-optical SAM presented here is complicated and difficult to use. However, most of this difficulty encountered in everyday use of this system stems from the need to align the optics, especially the relative positions of the generation and detection optics. In addition to this, the system is sensitive to

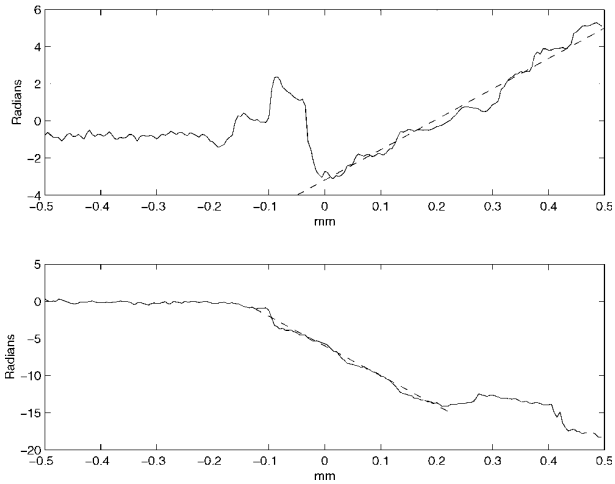

Figure 10. Graphs of unwrapped phase from figure 9. The upper graph shows the first scan line, the lower the last. In the upper graph the amplitude over the void is dominated by the A_0 mode and in the lower the S_0 mode dominates. The ripples in the phase indicate the presence of the other mode. Choosing a section of the data in which one mode dominates simplifies the interpretation of the data. The broken lines show the straight line fits to the data over the region of the subsurface void. These indicate a velocity difference (obtained using equation (2)) of -280 m s^{-1} for the upper graph and +700 m s^{-1} for the lower graph (these are not really 'small differences') which agrees with figure 11 (the upper graph corresponds to the left-hand side of figure 11, the lower to the right-hand side).

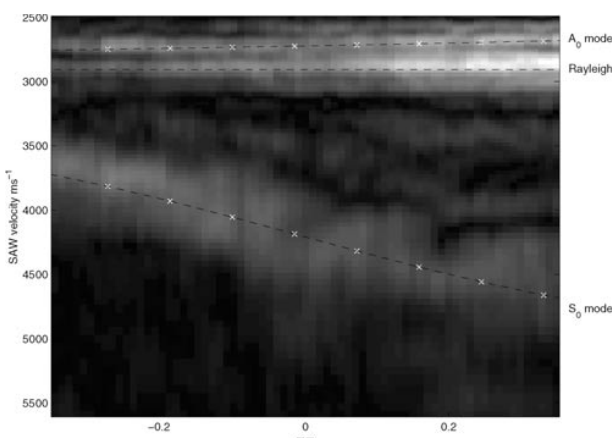

Figure 11. The velocity content of the complex amplitude shown in figure 9. The image is constructed by Fourier transforming the complex amplitude along the direction of propagation and then transforming the result to show velocity rather than spatial frequency. The reflected Rayleigh wave is weak and lost in noise and not shown here. The incoming Rayleigh mode and the two Lamb modes are clearly visible. The broken lines show the velocities for the Rayleigh and the Lamb modes. These lines were fitted to the data using the solutions for the Lamb wave velocities from [16]. The fit indicates a mean thickness of 28 μm and a variation in thickness of 6 ± 2 μm on going from left to right. This is consistent with the sample preparation conditions (figure 8).

the sample/material velocity and, while this is not a problem in principle, it does require additional adjustment of the optical system.

The next generation of all-optical SAMs, which is currently under construction, will utilize a spatial light modulator instead of computer generated holograms. While this sacrifices some flexibility in the optical design, it does allow the system to self-align and to self-select the best tailored distribution for any sample, thus removing the need for most alignment by the user.

7.1. Nonlinear imaging

This system will be a strong contender for the detection of material nonlinearities because its generation amplitude and detection sensitivity put it in the correct range for the detection of strong nonlinearity. The ability of the tailored distributions to filter and spatially separate generated frequency components is crucial to this type of experiment. While the focusing does not (overall) improve the nonlinear response, it does localize it to SAW point spread function. This is especially important for the detection of nonlinearities in coated and layered media, in which strong dispersion may be expected, which would prevent the build up of a nonlinear response over large distances.

7.2. Aberrations

Acoustic aberrations which can give rise to significant signal loss and acoustic speckle are a significant problem in many areas of ultrasonics. They are especially significant at high frequencies and in inhomogeneous materials such as polycrystalline metals. They are often restrict the upper frequency range of techniques before the intrinsic absorption of the material does [17]. However, with the use of *adaptive* techniques [17, 18] this can be compensated for. The next generation of our non-contact SAM utilizing a SLM will allow real-time adaptation of the generation source, which will allow the SAM to dynamically refocus the SAWs to compensate for acoustic aberrations, allowing the microscope to operate on a wide range of inhomogeneous materials over a wide frequency range.

8. Conclusion

This paper has shown that the major problem for an all-optical SAM is the signal shot SNR. This arises from the relative insensitivity of optical detection techniques (compared with contacting transducers). The usual techniques for overcoming the lack of signal, use of large generation powers and signal averaging, are not useful in the case of an all-optical SAM, which must be fast and damage free.

The use of tailored optical generation distributions is shown to improve the signal levels (by focusing the generated ultrasound) and to reduce surface damage (by spreading out the optical power). A simple expression for the improvement in signal levels gained by focusing over line source generation is presented.

Various methods for tailoring the optical distribution are discussed and the use of computer generated holograms and of spatial light modulators are selected as the two methods most suitable for producing tailored distributions for use in an all-optical SAM. A microscope based on these principles and using computer generated holograms is demonstrated.

It is capable of measurement rates of 2 kHz and is totally damage free. Imaging on aluminium and silicon nitride with a contrast resulting from amplitude and velocity changes and mode conversion is demonstrated. The possibilities for multiwavelength imaging and sectioning and for harmonic (nonlinear) imaging are discussed.

A new all-optical SAM is undergoing conversion using a SLM. This SAM will be used in measurement trials to demonstrate its effectiveness for a wide range of engineering applications and on a variety of materials, including steel and polymers. The use of the SLM will greatly simplify the operation of the non-contact SAM, because the generation profile will be automatically tailored in real time to produce the best SNR for the material being tested. This will also dispense with some of the more difficult operator tasks associated with these optical techniques by allowing the SAM to optically align itself for optimum performance on a wide range of materials and to switch between imaging modes and generation frequencies automatically. The SAM will also be able to operate on single-crystalline and multicrystal anisotropic materials by changing the generation profile to compensate for the anisotropy.

Acknowledgments

We would like to thank Victor Krylov, Department of Civil and Structural Engineering, Nottingham Trent University, UK and acknowledge the support of the UK Engineering and Physical Sciences Research Council (EPSRC) and Rolls Royce PLC.

References

[1] Lemons R A and Quate C F 1974 Acoustic microscope—scanning version *Appl. Phys. Lett.* **24** 163–5

[2] Parmon W and Bertoni H L 1979 Ray interpretation of the material signature of the acoustic microscope *Electron. Lett.* **15** 684–6

[3] Somekh M G, Bertoni H L, Briggs G A D and Burton N J 1985 A two-dimensional imaging theory of surface discontinuities with the scanning acoustic microscope *Proc. R. Soc.* A **401** 29–51

[4] Scruby C B and DrainN J 1990 *Laser Ultrasonics, Techniques and Applications* (Bristol: Hilger)

[5] Krylov V V, Ponomarev E P and Shtentsel T V 1986 Characteristics of thermooptic excitation of sound in metals *Vestnik Moskoskogo Universiteta, Fiz.* **41** 43–8 (Engl. Transl. 1986 *Moscow University Phys. Bull.* **41** 46–51)

[6] Stepanov S I 1994 Sensitivity of non-steady-state photoelectromotive force-based adaptive photodetectors and characterization techniques *Appl. Opt.* **33** 915–20

[7] Monchalin J P 1986 Optical detection of ultrasound *IEEE Trans. Ultrasonics, Ferroelectrics Frequency Control* **33** 485–99

[8] Dewhurst R J and Shan Q 1999 optical remote measurement of ultrasound *Meas. Sci. Technol.* **10** R139–68

[9] Born M and Wolf E 1964 *Principles of Optics* (Oxford: Pergamon)

[10] Nishino H, Tsukahara Y, Nagata Y and Yamanaka K 1993 Analysis of excitation and coherent amplitude enhancement of surface acoustic-waves by the phase-velocity scanning method. *Appl. Phys. Lett.* **62** 2036–8

[11] Cielo P, Jen C K and Maldague X 1985 The converging-surface-acoustic-wave technique—analysis and applications to nondestructive evaluation *Can. J. Phys.* **64** 55–62

[12] Cielo P and Jen C K 1987 Laser generation of convergent acoustic-waves and applications to materials evaluation *IEEE Trans. Ultrasonics, Ferroelectrics Frequency Control* **34** 396

[13] Clark M 1999 Two-dimensional, three-dimensional, and gray-scale images reconstructed from computer-generated holograms designed by use of a direct-search method *Appl. Opt.* **38** 5331–7

[14] Sharples S D, Clark M and Somekh M 1999 Noncontact continuous wavefront/diffractive acoustic elements for Rayleigh wave control. *Appl. Phys. Lett.* **74** 3604–6

[15] Clark M, Sharples S D and Somekh M 2000 Diffractive acoustic elements for laser ultrasonics. *J. Acoust. Soc. Am.* **107** 3179–85

[16] Viktorov I A 1967 *Rayleigh and Lamb Waves* (New York: Plenum)

[17] Clark M, Sharples S D and Somekh M 1999 Fast all optical Rayleigh wave microscope: imaging on isotropic and anisotropic materials *IEEE Trans. Ultrasonics, Ferroelectrics Frequency Control* **47** 65–74

[18] Clark M, Sharples S D and Somekh M G 1999 Saw imaging in anisotropic media *Proc. 1999 Review of Progress in QNDE* vol 19B (Melville, NY: American Institute of Physics) pp 1757–62